

## Measurement of the cross section for electron-impact ionization of $\text{Xe}^{6+}$ ions

D. C. Gregory and D. H. Crandall

Physics Division, Oak Ridge National Laboratory, Oak Ridge, Tennessee 37830

(Received 27 December 1982)

The absolute cross section for electron-impact ionization of  $\text{Xe}^{6+}$  has been measured from below threshold to 1500 eV with the Oak Ridge National Laboratory crossed-beams apparatus. Excitation of inner-shell electrons to autoionizing states is found to contribute up to a factor of 10 more than direct processes to the single-ionization cross section, and indirect effects dominate the measurement over the entire energy range studied. Good agreement is found with distorted-wave excitation calculations added to Lotz direct-ionization predictions.

### I. INTRODUCTION

Electron-impact excitation and ionization play important roles in understanding laboratory and astrophysical plasmas, especially where partially stripped ions provide diagnostic information in laboratory devices.<sup>1</sup> Recent investigations of electron-impact ionization of multiply charged ions have emphasized that several mechanisms contribute to the total cross section. Direct single ionization is, in some cases, overwhelmed by inner-electron excitation followed by autoionization (promotion of an inner-shell electron leaving two or more electrons in excited states with sufficient total energy to ionize).<sup>2</sup> Recombination resonances may complicate such features by extending the excitation-autoionization threshold to lower energies, and possibly smearing the normally sharp energy dependence observed for electron-impact excitation.<sup>3</sup> In addition, more than one electron may be removed from the target ion in a single-collision event,<sup>4</sup> either by direct multiple knock-off or by inner-shell ionization followed by autoionization.

The target ion of the present experiment  $\text{Xe}^{6+}$  was selected for its relatively simple electronic configuration  $4d^{10}5s^2$  and large number of inner-shell electrons. A detailed theoretical investigation of excitation-autoionization is feasible in this case, and the prominent role of  $d$  electrons in previous ionization studies<sup>5</sup> makes heavier elements such as xenon especially interesting. Finally, the present data extend the xenon isonuclear sequence which exhibits strong indirect effects in  $\text{Xe}^{3+}$  ionization.<sup>6</sup> The present experiment reports only cross sections for single ionization of  $\text{Xe}^{6+}$ , although multiple-ionization studies of other charge states of xenon have been carried out by Achenbach *et al.*<sup>7</sup> Distorted-wave calculations for several members of

the Cd isoelectronic sequence, including  $\text{Xe}^{6+}$ , are reported in the preceding paper by Pindzola *et al.*<sup>8</sup>

### II. EXPERIMENTAL METHOD

The crossed-beam apparatus used in the present experiment has been described in detail recently,<sup>6,9</sup> so only a brief overview will be given here. Figure 1 is an overhead view of the main interaction chamber. An ion beam from the ORNL-PIG ion source<sup>10</sup> enters the ultrahigh-vacuum chamber and is separately focused in the horizontal and vertical directions by one-dimensional Einzel lenses. A 45° electrostatic analyzer (charge purifier) removes from the primary beam any ions which have changed charge in collisions with background gas along the flight path from the ion source. After passing through the interaction region, ions enter the charge analyzer which separates beam components by

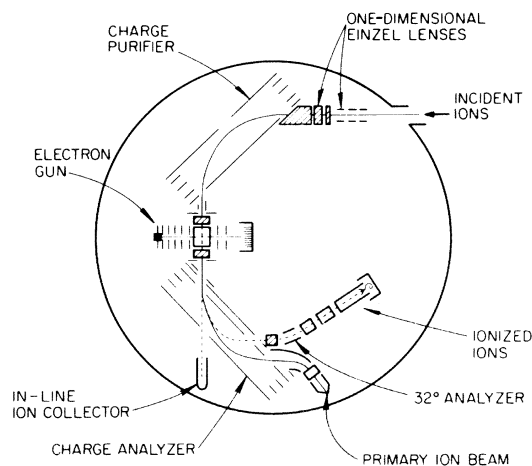


FIG. 1. Crossed-beams collision chamber viewed from above.

charge. This analyzer is designed specifically to separate a  $q = 6+$  parent ion beam from the further ionized  $q = 7+$  signal ions with minimum crosstalk. The primary ion beam is collected in a guarded Faraday cup while the signal ions are deflected and focused into a channeltron for counting. An in-line ion collector downstream from the interaction region is used for diagnostic tests.

TABLE I. Experimental electron-impact ionization cross sections for  $\text{Xe}^{6+}$ . Uncertainties are 1 s.d. (relative only).

Energy (eV)	Cross section ( $10^{-18} \text{ cm}^2$ )
88.8	0.35±0.60
90.6	-0.45±0.73
92.9	2.24±0.89
94.9	7.18±0.86
96.6	8.78±1.06
98.6	17.9 ±1.1
100.8	22.5 ±1.0
102.8	24.5 ±1.0
104.6	23.2 ±1.0
106.5	25.7 ±1.0
108.6	26.7 ±0.8
110.5	27.5 ±0.8
112.5	28.8 ±1.1
114.5	31.0 ±0.7
115.6	33.1 ±0.8
116.4	37.0 ±0.8
118.5	37.0 ±0.6
120.3	35.6 ±0.4
122.0	35.5 ±0.7
123.5	36.2 ±0.5
125.6	36.7 ±0.6
130.3	37.7 ±0.7
134.9	41.2 ±1.1
143	38.4 ±0.6
155	39.3 ±1.5
169	39.3 ±0.6
177	39.9 ±0.9
194	38.9 ±0.6
218	38.0 ±0.6
243	38.0 ±0.8
267	37.9 ±0.6
291	38.6 ±0.3
340	37.9 ±1.2
388	35.5 ±0.5
488	34.3 ±0.4
538	35.0 ±0.4
587	35.1 ±0.5
686	31.7 ±0.3
834	29.1 ±0.5
984	25.4 ±0.3
1230	22.9 ±0.6
1482	19.2 ±0.2

The electron gun, adapted from a design by Taylor *et al.*,<sup>11</sup> produces a magnetically confined beam from an indirectly heated cathode. Electrons are collected in a biased array of edge-on razor blades. The electron beam is chopped to allow separation of signal from background in the ion-signal channel. The penetration of stray electric fields into the collision volume has been reduced from previous experiments<sup>9</sup> so that the electron-beam energy spread is estimated to be approximately 1-eV full width at half maximum (FWHM) at energies near 100 eV. The vertical ion- and electron-beam spatial profiles are periodically measured at the collision volume and used to determine beam overlap integrals (form factors).

Relative uncertainties at the 1 s.d. level for each data point are listed in Table I and plotted with the data in Figs. 2 and 3. Uncertainties due to counting statistics and form-factor variations are combined in quadrature to obtain the relative uncertainty. In addition, the absolute magnitude of the cross section may be affected by factors common to all measurements. The channeltron efficiency<sup>12</sup> ( $0.98 \pm 0.02$ ) and pulse-processing efficiency ( $1.00 \pm 0.02$ ) combine to yield a signal-particle counting efficiency of  $0.98 \pm 0.03$  with uncertainty estimated at the equivalent of 90% confidence level for statistical uncertainties. Signal-particle transmission to the channeltron is assessed by monitoring signal strength while scanning each focusing and steering parameter along the signal channel and is estimated to be  $1.00 \pm 0.04$ . Ion and electron currents are accurate to  $\pm 2\%$  each, and the velocities are inferred to  $\pm 1\%$ . For a typical cross section value, the quadrature sum of all these systematic uncertainties with relative uncertainties at 90% confidence level (statistical  $\pm 3.2\%$  and form factor  $\pm 3\%$ ) yields a total absolute uncertainty of  $\pm 7.3\%$  at good confidence level near the peak cross section.

### III. RESULTS AND DISCUSSION

The complete data for electron-impact ionization of  $\text{Xe}^{6+}$  are listed in Table I and plotted in Fig. 2. The threshold for ionization of one of the ground-state  $5s^2$  electrons occurs at 90.7 eV,<sup>8</sup> and  $4d^{10}$  electrons may be directly ionized at 146 eV.<sup>13</sup> Ionization of further inner-shell electrons results in a highly excited  $\text{Xe}^{7+}$  ion which should autoionize to a higher charge state, so that the direct-single-ionization events which are observed result only from  $5s$  or  $4d$  electron removal.<sup>13</sup>

The one-parameter Lotz formula<sup>14</sup> provides a reasonable upper bound for direct-ionization cross sections in many cases,<sup>15</sup> although better agreement with experiment has been found if only half of the

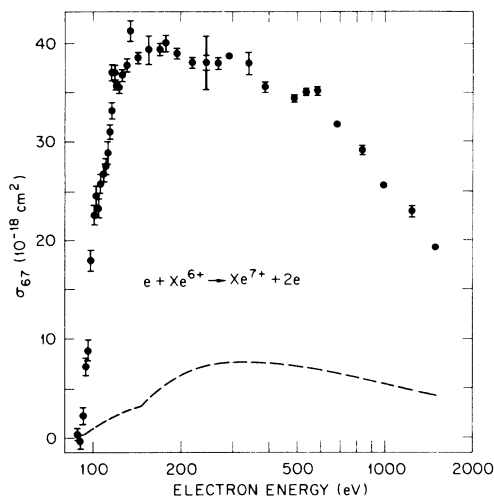


FIG. 2. Cross section for electron-impact ionization of  $\text{Xe}^{6+}$ . Relative uncertainties are plotted at the 1-s.d. level for each point, while the total absolute uncertainty ( $\pm 7.3\%$ ) at good confidence level (corresponding to 90% confidence for statistical uncertainties) is also shown at 240 eV. Dashed curve, Lotz prediction ( $4d$  contribution is divided by two).

calculated contribution from  $d$  electrons is used.<sup>6,16</sup> The Lotz prediction (with the  $4d$  contribution reduced by a factor of 2) is plotted in Fig. 2.

The experimental cross section begins to significantly exceed the Lotz prediction just above the ionization threshold. Based on similar comparisons in previous studies,<sup>2,6</sup> we conclude that the cross section is dominated by excitation-autoionization. The measurement is a factor of 10 higher than the Lotz prediction at 150 eV and is still a factor of 4 larger at 1500 eV. The indirect contribution obtained by subtracting the Lotz prediction for direct ionization from the measured cross section falls off as  $\ln E/E$  (where  $E$  is the electron energy) above 600 eV, which suggests that a substantial portion of the autoionizing states are reached through dipole-allowed transitions.<sup>17</sup> This is in contrast to recent measurements<sup>6</sup> on  $\text{Xe}^{3+}$ , where indirect ionization is observed only over a 100-eV energy range and is presumed to be due to nondipole-allowed transitions to autoionizing levels.

The observed energy dependence suggests that numerous transitions contribute to the overall excitation-autoionization effect observed in this experiment. The threshold region, expanded in Fig. 3, offers the best opportunity to observe the effects of individual transitions. Abrupt increases in the experimental cross section occur centered at 94, 98, and 116 eV. Specific  $4d-nl$  excitation cross sections

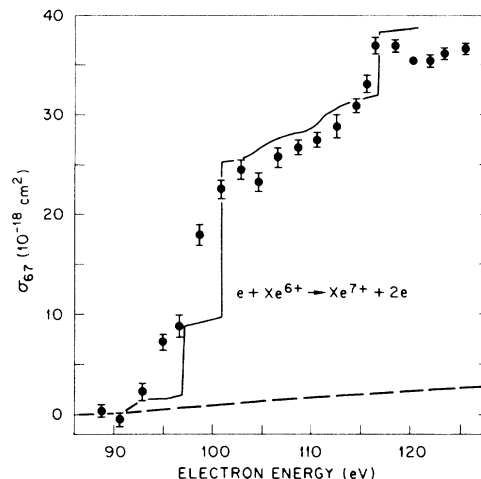


FIG. 3. Threshold region of the  $\text{Xe}^{6+}$  ionization cross section. Relative uncertainties are 1 s.d. Dashed curve, Lotz prediction; solid curve, distorted-wave excitation-autoionization theory (Ref. 8) added to Lotz.

have been calculated by Pindzola *et al.*<sup>8</sup> with threshold energies which correspond to these features. Excitation cross sections added to Lotz predictions produce the solid curve in Fig. 3. The calculations, employing unitarized distorted-wave theory including exchange and term-dependent wave functions, are in excellent agreement with our measurements, except that features in the 93–100-eV energy range appear in the experimental curve at lower energies than predicted. The shoulders observed below the calculated excitation thresholds could be due to dielectronic recombination resonances followed by double autoionization, which should smear the excitation onsets to lower energies.<sup>3</sup> A large number of weaker transitions to autoionizing levels account for the more gradual increases in the measured cross section, e.g., in the 106–116-eV range.

#### IV. CONCLUSIONS

Excitation-autoionization effects are found to be quite important in the ionization of  $\text{Xe}^{6+}$ , dominating the total single ionization over the entire energy range studied. The simple electron configuration and large indirect effects make this an excellent test for developing ionization theories which include indirect effects. Traditional calculations which ignore indirect effects will underestimate the cross section by up to a factor of 10.

#### ACKNOWLEDGMENTS

The technical assistance of J. Hale in daily operation of the ion source is gratefully acknowledged.

These measurements were suggested by D. C. Griffin and strongly encouraged by the related work of M. S. Pindzola, D. C. Griffin, and C. Bottcher. This research was supported by the Office of Fusion

Energy of the U. S. Department of Energy under Contract No. W-7405-eng-26 with Union Carbide Corporation.

- 
- <sup>1</sup>S. Suckewer, Phys. Scr. 23, 72 (1981).  
<sup>2</sup>R. A. Falk, G. H. Dunn, D. C. Griffin, C. Bottcher, D. C. Gregory, D. H. Crandall, and M. S. Pindzola, Phys. Rev. Lett. 47, 494 (1981).  
<sup>3</sup>K. J. LaGattuta and Y. Hahn, Phys. Rev. A 24, 785 (1981).  
<sup>4</sup>Alfred Müller and Reinhard Frodl, Phys. Rev. Lett. 44, 29 (1980).  
<sup>5</sup>H. P. Kelly, S. L. Carter, and B. E. Norum, Phys. Rev. A 25, 2052 (1982).  
<sup>6</sup>D. C. Gregory, P. F. Dittner, and D. H. Crandall, Phys. Rev. A 27, 724 (1983).  
<sup>7</sup>C. Achenbach, A. Müller, and E. Salzborn (private communication).  
<sup>8</sup>M. S. Pindzola, D. C. Griffin, and C. Bottcher, Phys. Rev. A 27, 2331 (1983).  
<sup>9</sup>D. H. Crandall, R. A. Phaneuf, R. A. Falk, D. S. Belić, and G. H. Dunn, Phys. Rev. A 25, 143 (1982).  
<sup>10</sup>M. L. Mallory and D. H. Crandall, IEEE Trans. Nucl. Sci. NS-23, 1069 (1976).  
<sup>11</sup>P. O. Taylor, K. T. Dolder, W. E. Kauppila, and G. H. Dunn, Rev. Sci. Instrum. 45, 538 (1974).  
<sup>12</sup>D. H. Crandall, J. A. Ray, and C. Cisneros, Rev. Sci. Instrum. 46, 562 (1975).  
<sup>13</sup>D. C. Griffin (private communication).  
<sup>14</sup>W. Lotz, Z. Phys. 216, 241 (1968).  
<sup>15</sup>D. H. Crandall, R. A. Phaneuf, and D. C. Gregory, Oak Ridge National Laboratory Report No. ORNL/TM-7020 (unpublished).  
<sup>16</sup>W. T. Rogers, G. Stefani, R. Camilloni, G. H. Dunn, A. Z. Msezane, and R. J. W. Henry, Phys. Rev. A 25, 737 (1982).  
<sup>17</sup>W. D. Robb, *Atomic and Molecular Processes in Controlled Thermonuclear Fusion* (Plenum, New York, 1980), pp. 245–265.